

Microwave Spectrum, Conformational Equilibrium, Intramolecular Hydrogen Bonding, Dipole Moments, ^{14}N Nuclear Quadrupole Coupling Constants and Centrifugal Distortion Constants of (Aminomethyl)cyclopropane

K.-M. MARSTOKK and HARALD MØLLENDAL

Department of Chemistry, The University of Oslo, P.O. Box 1033, Blindern, N-0315 Oslo 3, Norway

The microwave spectrum of (aminomethyl)cyclopropane has been investigated in the 18.0–29.0 GHz spectral range at about -50°C . The two heavy-atom *gauche* conformations denoted I and II were assigned. Both these conformations are stabilized by intramolecular hydrogen bonding. The internal energy difference, $\Delta E_0^0 = E_{\text{II}}^0 - E_{\text{I}}^0$, is 0.1(2) kJ/mol. (I is thus slightly more stable than II). The two assigned conformations I and II are each at least 3 kJ/mol more stable than any further conformation.

The heavy-atom dihedral angles are $59(3)^\circ$ from *anti* in I, and $62(3)^\circ$ from *anti* in II, respectively. The CCN angle has a “normal” value of $110.0(15)^\circ$ in I, while this angle opens up to $116.0(15)^\circ$ in II.

Three vibrationally excited states belonging to two different normal modes were assigned for each of the two rotamers. The vibrational frequencies were determined by relative intensity measurements.

The dipole moments are $\mu_a = 0.144(2)$ D, $\mu_b \sim 0$ D, $\mu_c = 1.068(16)$ D, and $\mu_{\text{tot}} = 1.077(16)$ D for I; $\mu_a = 1.018(26)$ D, $\mu_b = 0.39(16)$ D, $\mu_c = 0.833(55)$ D, and $\mu_{\text{tot}} = 1.372(60)$ D for II, respectively.

^{14}N nuclear quadrupole coupling constants of conformation I are $\chi_{aa} = 1.84(27)$ MHz and $\chi_{bb} = 2.34(17)$ MHz. It was not possible to determine these constants for II.

The conformational preferences of (aminomethyl)cyclopropane can be explained in accord with the Walsh model for cyclopropane.

The conformational properties of several methylcyclopropane derivatives

$(\text{CH}_2-\text{CH}_2-\text{CH}-\text{CH}_2\text{X})$ have recently been studied by electron diffraction and spectroscopic methods.¹ These molecules prefer the heavy-atom *gauche* or *syn* conformations depicted in Fig. 1. (Chloromethyl)cyclopropane^{1–3} and (bromomethyl)cyclopropane³ both exist as a mixture of *gauche* and *syn* in the gaseous state. The *gauche* forms are the more stable ones in these two molecules.^{1–3}

(Hydroxymethyl)cyclopropane has been found to exist only in the heavy-atom *gauche* conformation in the free state.⁴ Moreover, the hydroxyl hydrogen atom of this conformation is oriented in such a way that a weak intramolecular hydrogen bond is formed between this atom and the “quasi- π ” electrons of the cyclopropane ring as shown by Brooks *et al.*⁴

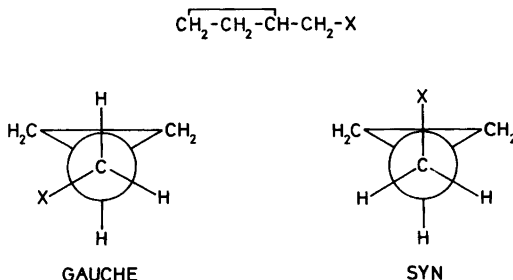


Fig. 1. Heavy-atom *gauche* and *syn* conformations normally found for methylcyclopropane derivatives.

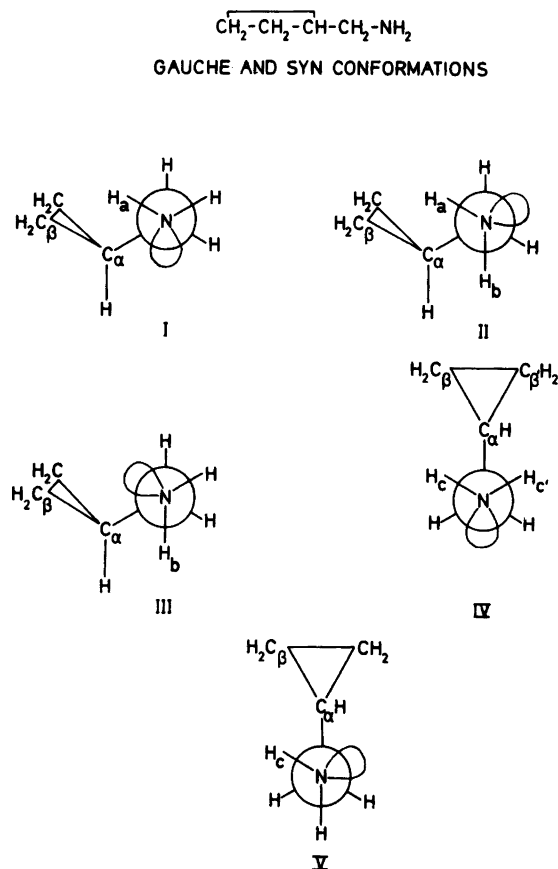


Fig. 2. Five typical, all-staggered conformations of (aminomethyl)cyclopropane viewed along the N-C bond. I and II were found together to make up at least 85 % of the gas at -50°C . I is more stable than II by $0.1(2)\text{kJ/mol}$.

Five typical conformations of (aminomethyl)cyclopropane are shown in Fig. 2. I, II and III are heavy atom *gauche* conformations (see Fig. 1), while IV and V are *syn* forms. The lone electron pair of the nitrogen atom is drawn as a lobe in Fig. 2.

According to the Walsh model of cyclopropane,⁵ the maximum electronic density of the quasi- π electrons are found in the plane of the ring on its outside. Hydrogen bonding is thus possible for all the five conformations shown in Fig. 2. The amino group hydrogen atom which could be engaged in intramolecular hydrogen bonding is denoted H_a , H_b , H_c or H_c' in this figure, while the plain symbol H is used for the amino group hydrogen atom not participating in hydrogen bonding.

This study was undertaken in order to investigate the conformational preferences of (aminomethyl)cyclopropane, thereby hoping to get an idea of which forces are responsible for its conformational choices. It was found that I and II predominate and together make up at least 85 % of the gas at about -50°C .

An infrared spectroscopic investigation including matrix isolation of this compound has now been initiated at this department by Mr. Geir Braathen.

EXPERIMENTAL

(Aminomethyl)cyclopropane was purchased from Fluka, A.G., Buchs, Switzerland and purified by gas chromatography before use. Studies

were made in the 18.0 to 29.0 GHz spectral region with the cell cooled with dry ice to about -50°C . Lower temperatures could not be used because of insufficient vapour pressure of the compound. The spectrum was recorded at pressures in the 0.2–2.0 Pa range. Free-running klystrons were employed as radiation sources. With this equipment, quadrupole fine structure splittings larger than about 0.6 MHz were resolved.

The microwave spectrum of (aminomethyl)cyclopropane is dense with absorptions occurring practically everywhere. The most intense lines are of moderate strengths. The peak absorption coefficients of the strongest transitions observed were roughly $5 \times 10^{-7} \text{ cm}^{-1}$ at about -50°C .

RESULTS

Assignment of the ground vibrational state of conformation I. Preliminary rotational constants of I were computed by combining structural parameters taken from related compounds. Bond moment calculations of the dipole moment were then performed using the values of Ref. 6. The results were: $\mu_a=0.3 \text{ D}$, $\mu_b=0.4 \text{ D}$, and $\mu_c=1.2 \text{ D}$. Searches were therefore first made for the strong *c*-type, *Q*-branch $K_{-1}=1 \rightarrow 2$ transitions, which were soon identified by their Stark effects, rigid-rotor fit, and more or less well-resolved quadrupole fine structure caused by the ^{14}N -nucleus. Assignments were then successively extended to include higher and higher values of *J* for the various *c*-type, *Q*-branch series transitions occurring in the investigated spectral range. Allowance had to be made for centrifugal distortion in this process. The maximum *J* value definitely assigned was 79 for the $79_{8,71} \rightarrow 79_{9,71}$ transition. Its peak intensity was roughly $2 \times 10^{-8} \text{ cm}^{-1}$. Transitions with even higher values of *J* were searched for, but not identified with certainty, presumably because of insufficient intensities.

There are only few low-*J*, *c*-type, *R*-branch lines in the spectrum, and they were first identified after the assignment of conformation II had been made as described below. The assignments of the *R*- and *P*-branch lines were then successively extended to high values of *J* and K_{-1} in the same manner as described for the *Q*-branch transitions. Maximum values of *J* and K_{-1} (for the coalescing K_{-1} doublets) were $69_{22} \rightarrow 70_{21}$ for the *R*, and $70_{24} \rightarrow 69_{25}$ for the *P*-branch transitions. A total number of about 180 *c*-type transitions were

assigned for the ground vibrational state of conformation I. 45 selected transitions are shown in Table 1. (The complete microwave spectra of I and II as well as their vibrationally excited states are available from the authors upon request or from Molecular Spectra Data Center, Bldg. 221, Room B 265, National Bureau of Standards, Washington D.C. 20234, U.S.A., where they have been deposited.) 164 transitions were used to derive the spectroscopic constants displayed in Table 2. The low-*J* lines which were split by quadrupole coupling between the ^{14}N nucleus and the overall rotation, were included in the final fit after allowance had been made for this effect in the manner to be described in the section on quadrupole coupling.

As shown in Table 2, accurate values were found for the quartic, while the four sextic constants used in the fit are of a rather poor quality.

The spectroscopic constants of Table 2 very accurately predict the frequencies of hypothetical *a*- and *b*-type transitions. However, none of these were definitely identified presumably because of insufficient intensities caused by small *a*- and *b*-axis dipole moment components. This is in keeping with the fact that $\mu_a=0.144(2) \text{ D}$ and $\mu_b \sim 0 \text{ D}$, as will be shown below in the section on dipole moment determination.

Vibrationally excited states of I. The ground state transitions were accompanied by a satellite spectrum presumably belonging to vibrationally excited states of conformation I. The strongest of these satellites had about 35 % of the ground state intensity at about -50°C . Relative intensity measurements performed largely as prescribed in Ref. 7 yielded $159(20) \text{ cm}^{-1}$ for this vibration, which is assumed to be the C–C torsional fundamental.

A total of about 130 transitions were measured for this vibrationally excited state, and 114 of these were used to determine the spectroscopic constants appearing in Table 2. Maximum value for *J* for the *Q*-branch lines was found for the $78_{8,70} \rightarrow 78_{9,70}$ transition. For the *R*-branch, the $56_{18} \rightarrow 57_{17}$ coalescing K_{-1} -pair and for the *P*-branch, the $58_{20} \rightarrow 57_{21}$ coalescing transitions involved the maximum *J*-values, respectively.

Apart from its intensity, the observed changes of the rotational constants upon excitation also indicate that this is indeed the first excited state of the C–C torsional vibration. The observed

Table 1. Selected transitions for the ground vibrational state of conformation I of (aminomethyl)-cyclopropane.

Transition	Observed frequency ^a (MHz)	Obs.-calc. frequency (MHz)	Centrifugal Total (MHz)	Distortion Sextic (MHz)
1 _{0,1} → 2 _{1,1}	21901.08	-0.03	-0.05	
2 _{0,2} → 3 _{1,2}	28478.84	-0.01	-0.15	
2 _{1,1} → 2 _{2,1}	27267.85	-0.09	-0.22	
3 _{1,2} → 3 _{2,2}	26768.18	0.01	-0.11	
4 _{1,3} → 4 _{2,3}	26105.78	-0.01	0.06	
5 _{1,4} → 6 _{0,6}	24057.48	0.06	-0.66	
6 _{1,5} → 7 _{0,7}	28698.17	-0.06	-0.89	
7 _{1,6} → 7 _{2,5}	23190.18	-0.03	1.13	
9 _{1,8} → 9 _{2,8}	20555.74	-0.02	2.52	
9 _{2,8} → 10 _{1,10}	23108.05	0.01	-2.25	
9 _{4,5} → 8 _{5,3}	28549.90	0.09	-2.95	
9 _{4,6} → 8 _{5,4}	28552.52	-0.13	-2.95	
13 _{4,9} → 14 _{3,11}	22349.84	-0.04	-16.17	
16 _{5,11} → 17 _{4,13}	21311.63	-0.02	-25.35	0.01
16 _{5,12} → 17 _{4,14}	20893.80	0.05	-23.76	0.01
18 _{2,16} → 18 _{3,16}	28730.45	0.05	26.29	-0.02
19 _{6,13} → 20 _{5,15}	20844.35	0.01	-38.53	0.03
19 _{6,14} → 20 _{5,16}	20757.61	-0.01	-37.95	0.03
22 _{2,20} → 22 _{3,20}	18916.03	0.03	44.27	-0.04
23 _{7,16} → 24 _{6,18}	26829.93	0.00	-67.20	0.06
23 _{7,17} → 24 _{6,19}	25802.70	0.10	-66.89	0.06
29 _{3,26} → 29 _{4,26}	28597.69	-0.01	130.67	-0.22
32 _{3,29} → 32 _{4,29}	19504.42	0.05	150.62	-0.28
39 _{4,35} → 39 _{5,35}	28530.63	-0.03	348.14	-0.93
49 _{5,44} → 49 _{6,44}	26928.71	0.04	708.75	-2.76
58 _{6,52} → 58 _{7,52}	28384.18	0.01	1254.01	-6.59
68 _{7,61} → 68 _{8,61}	25399.03	-0.05	1930.52	-13.42
70 _{7,63} → 70 _{8,63}	18352.11	-0.04	1673.56	-12.12
77 _{8,69} → 77 _{9,69}	26172.29	0.02	2903.37	-25.37
78 _{8,70} → 78 _{9,70}	22322.21	0.06	2696.75	-23.99
79 _{8,71} → 79 _{9,71}	18898.07	-0.03	2474.10	-22.42
Coalescing K_{-1} -doublet lines ^b				
15 ₆ → 14 ₇	29003.85	0.06	-0.90	
19 ₇ → 18 ₈	23083.12	-0.06	9.65	
28 ₁₀ → 27 ₁₁	23741.80	0.06	46.96	-0.06
34 ₁₂ → 33 ₁₃	24196.94	0.00	93.92	-0.18
40 ₁₄ → 39 ₁₅	24672.29	0.06	163.66	-0.46
49 ₁₇ → 48 ₁₈	25434.18	0.01	320.48	-1.39
56 ₁₉ → 55 ₂₀	19860.99	-0.03	525.27	-3.08
67 ₂₃ → 66 ₂₄	27192.35	0.02	874.95	-7.32
70 ₂₄ → 69 ₂₅	27522.19	0.01	1004.71	-9.21
31 ₁₀ → 32 ₉	19776.66	0.02	-141.25	0.26
38 ₁₂ → 39 ₁₁	25481.15	-0.09	-257.95	0.71
46 ₁₅ → 47 ₁₄	18458.44	0.09	-419.29	1.72
56 ₁₈ → 57 ₁₇	23739.90	-0.02	-752.74	4.54
66 ₂₁ → 67 ₂₀	28882.23	-0.08	-1226.71	10.24
69 ₂₂ → 70 ₂₁	28516.32	0.07	-1388.69	12.69

^a ±0.10 MHz. Transitions with resolved quadrupole splittings have been "corrected" for this effect. The quadrupole splittings can be computed using the quadrupole coupling constants of Table 4.^b The K_{-1} -energy doublets coalesce for high values of K_{-1} . Subscripts of J -quantum number refer only to K_{-1} .

Table 2. Spectroscopic constants for conformation I of (aminomethyl)cyclopropane. ^a

Vibrational state	Ground	First ex. C-C tors.	Second ex. C-C tors.
No. of transitions	164	114	46
Rms (MHz) ^b	0.0609	0.0753	0.1734
A_v (MHz)	12292.3316(51)	12274.7647(85)	12258.519(28)
B_v (MHz)	3202.9457(14)	3196.7573(22)	3190.1038(86)
C_v (MHz)	2865.8045(12)	2864.1778(21)	2862.3134(84)
Δ_J (kHz)	1.1426(53)	1.1360(98)	0.970(36)
Δ_{JK} (kHz)	-4.262(50)	-3.744(92)	-4.79(30)
Δ_K (kHz)	21.246(28)	20.280(54)	21.06(14)
δ_J (kHz)	0.20242(35)	0.19553(63)	0.1880(28)
δ_K (kHz)	2.506(68)	2.69(12)	0.39(76)
H_J (Hz)	-0.00044(21)	-0.00077(80)	-0.00339(52)
H_{JK} (Hz)	-0.0341(12)	-0.0260(29)	-0.088(13)
H_{KJ} (Hz)	-0.062(30)	-0.13(11)	- ^d
H_K (Hz) ^c	0.250(89)	0.44(31)	- ^d

^a Uncertainties represent one standard deviation. ^b Rms is the root-mean-square deviation. ^c Further sextic constants kept at zero in least-squares fit. ^d Kept at zero in least-squares fit.

changes were $\Delta A = -17.57$ MHz, $\Delta B = -6.19$ MHz, and $\Delta C = -0.38$ MHz, as compared to $\Delta A = -17.52$ MHz, $\Delta B = -4.32$ MHz and $\Delta C = -2.23$ MHz found by decreasing the heavy-atom dihedral angle of the plausible structure (see below) by 0.5° from *syn*.

The second vibrationally excited state of the C-C torsion was also assigned and the spectroscopic constants displayed in Table 2, were determined. About 60 lines were identified and 46 of them used in the least squares fit. In this case, $60_{6,54} \rightarrow 60_{7,54}$ was the maximum *J*, *Q*-branch; $50_{16} \rightarrow 51_{15}$ the maximum *J*, *R*-branch and $46_{16} \rightarrow 45_{17}$ the maximum *J*, *P*-branch transitions. None of the lines were split by other effects than quadrupole coupling.

It can be seen from Table 2 that the changes of the rotational constants upon excitation of the C-C torsional mode varies nearly linearly through its two first excited states. This is typical for a harmonic mode.

The third excited state of the C-C torsional frequency could not be found because its intensity is so low; roughly 5 % of that of the ground state.

17 *Q*-branch lines of the *c*-type variety with a maximum *J* value of 59 (for the $59_{6,53} \rightarrow 59_{7,53}$ transition) were assigned for a third excited state having about 20 % of the intensity of the ground state. Relative intensity measurements⁷ yielded $259(30)$ cm⁻¹ for this fundamental vibration. A

tentative assignment was made for one *R*-branch line, but this assignment could not be confirmed due to the crowded nature of this spectrum. The tentative rotational constants not included in Table 2 are: $A = 12319.378(92)$ MHz, $B = 3196.796(28)$ MHz and $C = 2860.557(24)$ MHz. Ray's asymmetry parameter $\kappa = -0.928905$ as well as $A - C = 9458.821(95)$ MHz are definite, however.

Due to its frequency of $259(30)$ cm⁻¹, two assignments of this mode appear possible. It could be the C-N torsional mode or the C-C-N bending mode. Increase of this angle in the plausible model of Table 8 by 0.5° led to an increase of $A - C$ by about 31 MHz. This is close to the experimental value as can be seen from Table 2 and the results just quoted. Furthermore, the C-N torsional mode is expected to produce a smaller change in $A - C$ upon excitation than the observed one, because little reduced mass is involved in this motion. Thus, there can be no doubt that the *Q*-branch lines of the first excited state of the C-C-N bending mode has been assigned.

Attempts were also made to assign the first excited state of the C-N torsional mode. This mode has a frequency of about 350 cm⁻¹ in the related internal hydrogen-bonded compound CH₂FCH₂NH₂.⁸ An intensity of roughly 10 % of that of the corresponding ground state lines was expected for this vibrationally excited state.

However, searches among the rather few unassigned lines of medium intensity were inconclusive.

Dipole moment of I. The Stark coefficients shown in Table 3 were used to determine the dipole moment using standard procedure.⁸ Relatively large Stark splittings were measured in order to minimize complications from ¹⁴N quadrupole interaction. The standard deviation assigned to the observed Stark coefficients of Table 3 are presumed to take possible ¹⁴N quadrupole interaction into account.

Initially, all three dipole moment components were fitted. However, μ_b was then found to have an imaginary value. In the final fit which is reported in Table 3, μ_b was preset at zero.

There is the expected agreement between the observed dipole moment principal axes components (Table 3) and those predicted using the bond moment method (see above). This is independent evidence for the fact that the observed rotamer is indeed conformation I.

¹⁴N quadrupole coupling constants of I. Many lines were split due to quadrupole coupling of the ¹⁴N nucleus with the molecular rotation. The procedure of Ref. 8 was used to determine χ_{aa} and χ_{bb} reported in Table 4. The split frequencies were then "corrected" using these quadrupole coupling constants and used in the final least squares fit with the results shown in Tables 1 and 2. Quadrupole coupling for vibrationally excited states were assumed to be identical to the ground state values in the computations of the spectroscopic constants reported in Table 2.

Table 3. Stark coefficients^a and dipole moment of conformation I of (aminomethyl)cyclopropane.

Transition		$\Delta\nu/E^2$ (MHzV ⁻² cm ²) $\times 10^6$	
		Obs.	Calc.
3 _{1,2} →3 _{2,2}	M =2	-10.2(2)	-9.18
	M =3	-22.9(3)	-23.92
2 _{0,2} →3 _{1,2}	M=0	-6.37(8)	-6.29
	M =1	-2.11(3)	-2.14
	M =2	10.4(2)	10.34

Dipole moment^b

$$\mu_a=0.144(2) \text{ D}; \mu_c=1.068(16) \text{ A}; \mu_{tot}=1.077(16) \text{ D}$$

^a Uncertainties represent one standard deviation.

^b μ_b assumed to be zero. See text.

Table 4. ¹⁴N quadrupole splittings^a and diagonal elements of the quadrupole coupling tensor of conformation I of (aminomethyl)cyclopropane.

Transition	F→F'	E _q (obs.) (MHz)	E _q (obs.) - E _q (calc.) (MHz)
3 _{1,3} →3 _{2,1}	4→4	0.49(3)	0.08
	3→3	-1.19(3)	0.05
4 _{1,3} →4 _{2,3}	5→5	-0.15(5)	0.07
	4→4	0.61(4)	0.02
5 _{1,4} →5 _{2,4}	6→6	-0.19(5)	0.06
	5→5	0.55(4)	-0.10
6 _{1,5} →6 _{2,5}	7→7	-0.23(4)	0.04
	6→6	0.58(3)	-0.10
7 _{1,6} →7 _{2,6}	8→8	-0.27(4)	0.02
	7→7	0.70(3)	0.01
8 _{1,7} →8 _{2,7}	9→9	-0.22(3)	0.07
	8→8	0.76(3)	0.07
9 _{1,8} →9 _{2,8}	10→10	-0.15(3)	0.14
	9→9	0.70(3)	0.02
10 _{1,9} →10 _{2,9}	11→11	-0.20(3)	0.09
	10→10	0.80(3)	0.13
1 _{0,1} →2 _{1,1}	2→3	0.25(4)	-0.01
	1→2	-0.91(4)	0.14
2 _{0,2} →3 _{1,2}	2→3	-1.04(3)	-0.09
	3→4	0.26(3)	-0.03
4 _{1,3} →5 _{0,5}	1→2	0.81(5)	-0.05
	4→5	1.06(4)	0.00
5 _{1,4} →6 _{0,6}	6→7	-0.38(5)	0.06
	5→6	1.24(3)	0.14
6 _{1,5} →7 _{0,7}	7→8	-0.53(5)	-0.06
	6→7	1.12(3)	-0.04

Quadrupole coupling constants

$$\chi_{aa}=1.84(27) \text{ MHz}; \chi_{bb}=2.34(17) \text{ MHz.}$$

^a Uncertainties represent one standard deviation.

Assuming the principal nuclear axis quadrupole coupling constant χ_z to be -4.1 MHz as found in NH₃^{9a} and to be oriented 109.47° with respect to both N-H bonds, χ_{aa} and χ_{bb} were calculated to be 1.9 MHz and 2.0 MHz using the formula of Ref. 9b. This is close to the experimental values of Table 4 (1.84(27) MHz and 2.34(17) MHz, respectively) and is another evidence for the assignment of this rotamer as conformation I.

Assignment of the ground vibrational state of conformation II. Previous works^{10,11} indicate that conformations I and II ought to occur with roughly the same energy. The rotational constants of II were then predicted as were the

Table 5. Selected transitions for the ground vibrational state of conformation II of (aminomethyl)-cyclopropane.

Transition frequency ^a	Observed frequency (MHz)	Obs.-calc. (MHz)	Total Centrifugal distortion (MHz)	Sextic (MHz)
a-type				
2 _{0,2} → 3 _{0,3}	17995.68	0.00	-0.12	
2 _{1,1} → 3 _{1,2}	18496.89	0.02	-0.13	
3 _{0,3} → 4 _{0,4}	23956.33	0.00	-0.27	
3 _{1,2} → 4 _{1,3}	24652.45	-0.07	-0.32	
3 _{1,3} → 4 _{1,4}	23390.03	-0.01	-0.18	
3 _{2,1} → 4 _{2,2}	24112.68	0.09	-0.18	
3 _{2,2} → 4 _{2,3}	24031.37	0.02	-0.16	
b-type				
2 _{0,2} → 3 _{1,3}	26252.37	0.00	-0.04	
4 _{1,4} → 5 _{0,5}	22194.77	-0.08	-0.67	
3 _{1,3} → 3 _{2,2}	28457.59	-0.11	-0.24	
4 _{1,4} → 4 _{2,3}	29099.13	0.13	-0.22	
5 _{1,4} → 5 _{2,3}	25454.82	0.11	0.18	
7 _{1,6} → 7 _{2,5}	24206.10	0.02	0.61	
9 _{1,8} → 9 _{2,7}	23253.69	-0.07	0.89	
11 _{1,10} → 11 _{2,9}	23000.84	-0.04	0.48	
13 _{1,12} → 13 _{2,11}	23785.19	0.01	-1.43	
16 _{1,15} → 16 _{2,14}	27442.59	-0.01	-9.50	
10 _{0,10} → 10 _{1,9}	20488.81	0.13	-3.56	
12 _{0,12} → 12 _{1,11}	26184.06	0.05	-7.39	
c-type				
1 _{0,1} → 2 _{1,1}	21661.08	-0.02	-0.06	
2 _{0,2} → 3 _{1,2}	28147.27	0.04	-0.16	
4 _{1,3} → 4 _{2,3}	25941.60	-0.06	0.03	
5 _{1,4} → 6 _{0,6}	24014.55	0.07	-0.65	
6 _{1,5} → 7 _{0,7}	28705.12	0.00	-0.90	
7 _{1,6} → 7 _{2,6}	23203.39	-0.03	1.02	
10 _{1,9} → 10 _{2,9}	19316.85	-0.02	3.18	
13 _{4,9} → 14 _{3,11}	21860.75	-0.06	-15.07	
13 _{4,10} → 14 _{3,12}	20382.43	0.06	-12.30	
19 _{2,17} → 19 _{3,17}	27329.27	-0.08	28.65	-0.03
30 _{3,27} → 30 _{4,27}	27791.90	-0.02	133.93	-0.26
41 _{4,37} → 41 _{5,37}	25210.02	0.00	358.45	-1.13
50 _{5,45} → 50 _{6,45}	28119.13	-0.06	722.98	-3.24
60 _{6,54} → 60 _{7,54}	26741.10	-0.07	1259.73	-7.75
71 _{7,64} → 71 _{8,64}	21333.80	0.04	1834.78	-15.15
80 _{8,72} → 80 _{9,72}	22881.77	-0.03	2789.05	-28.74
Coalescing K_{-1} doublet lines^b				
16 ₆ → 15 ₇	22694.68	-0.02	2.87	
28 ₁₀ → 27 ₁₁	23607.33	0.02	41.31	-0.10
37 ₁₃ → 36 ₁₄	24322.45	0.05	112.37	-0.41
47 ₁₆ → 46 ₁₇	19018.30	0.00	274.29	-1.46
55 ₁₉ → 54 ₂₀	25908.15	0.09	421.45	-3.15
58 ₂₀ → 57 ₂₁	26198.82	-0.06	500.34	-4.13
32 ₁₀ → 33 ₉	25559.32	-0.05	-151.27	0.30
43 ₁₄ → 44 ₁₃	18336.05	0.03	-323.37	1.22
53 ₁₇ → 54 ₁₆	23563.14	0.09	-601.05	3.39
59 ₁₉ → 60 ₁₈	22923.94	-0.02	-809.81	5.71

^a ±0.10 MHz. ^b Comments as for Table 1.

dipole moment components. They were calculated as $\mu_a=0.6$ D, $\mu_b=0.8$ D, and $\mu_c=1.0$ D, respectively, using the bond moment method.⁶ Search was therefore first made for *c*-type *Q*-branch lines which were soon found and used to locate the weaker *b*-type, *Q*-branch transitions. A line at 28147.27 MHz had a very characteristic Stark effect and was immediately assigned as the $2_{0,2} \rightarrow 3_{1,2}$ transition. Further *a*- and *c*-type low *J*, *R*-branch lines were then identified with ease. The assignment was now extended to high values of *J* in the same manner as described for conformation I. Maximum value for *J* was found for the $80_{8,72} \rightarrow 80_{9,72}$ *Q*-branch transition. The $58_{20} \rightarrow 57_{21}$ and $59_{19} \rightarrow 60_{18}$ transitions had the maximum value of *J* for the *R* and *P*-branch transitions, respectively.

A selected portion of the spectrum is listed in Table 5. A total of about 170 transitions were assigned and 151 of them used to determine the spectroscopic constants shown in Table 6. Very accurate values were derived for the quartic centrifugal distortion constants, while the four sextic constants hardly have much physical significance (see Table 6).

Vibrationally excited states of II. The spectra of the vibrationally excited states of II were quite similar to the corresponding ones found for conformation I, and the same three vibrationally excited states were assigned in both cases as seen from Tables 2 and 6.

The C–C torsional frequency was found to be $148(20)$ cm^{-1} by relative intensity measurements.⁷ This is similar to the above-found values for I, as expected. The changes of the rotational constants are also similar to those found for I as can be seen from Tables 2 and 6, and these changes are again fairly well reproduced by increasing the heavy-atom dihedral angle of the plausible structure (see later section) by 0.5° .

Maximum value of *J* for the *c*-type *Q*-branch lines was found for the $62_{6,56} \rightarrow 62_{7,56}$ transition. For the *R*-branch, the $50_{16} \rightarrow 51_{15}$ coalescing transitions, and for the *P*-branch, the $43_{15} \rightarrow 42_{16}$ transitions involved the maximum *J*-values, respectively, of the first excited C–C torsional state.

The second excited state (Table 6) of the C–C torsional mode together with the first excited state indicate that this mode is quite harmonic for similar reasons as discussed for I.

In the case of the second excited state of the C–C torsion, no high *J*, *P* or *R*-branch lines were identified, presumably because of lack of intensity, while the $51_{5,46} \rightarrow 51_{6,46}$ involved the maximum *J* found for the *Q*-branch lines.

Finally, a tentative assignment was made for the first excited state of the lowest heavy-atom bending mode. The rotational constants (not reported in Table 6) were found as $A=12207.056(82)$ MHz, $B=3156.884(33)$ MHz and $C=2840.522(32)$ MHz, with $\kappa=-0.932449$,

Table 6. Spectroscopic constants for conformation II of (aminomethyl)cyclopropane.^a

Vibrational state No. of transitions Rms (MHz) ^b	Ground 151 0.0633	First ex. C–C tors. 93 0.0734	Second ex. C–C tors. 17 0.1890
A_v (MHz)	12173.1806(50)	12151.8496(86)	12137.87(15)
B_v (MHz)	3162.6582(13)	3157.4117(21)	3152.508(43)
C_v (MHz)	2846.8065(12)	2845.3493(19)	2843.611(54)
Δ_J (kHz)	1.1254(25)	1.1014(44)	1.4(17)
Δ_{JK} (kHz)	-3.749(23)	-3.640(38)	-4.8(16)
Δ_K (kHz)	20.868(14)	20.329(33)	147(43)
δ_J (kHz)	0.18659(27)	0.17867(49)	0.095(20)
δ_K (kHz)	2.646(49)	2.768(98)	23.3(39)
H_J (Hz)	-0.00039(68)	-0.0023(21)	- ^d
H_{JK} (Hz)	-0.0369(18)	-0.0236(58)	- ^d
H_{KJ} (Hz)	-0.013(87)	-0.33(28)	- ^d
H_K (Hz) ^c	0.032(249)	0.89(79)	- ^d

^{a,b,c,d} Comments as for Table 2.

from 12 definitely assigned *Q*-branch lines and 1 suspected, but not confirmed, *R*-branch transition. Relative intensity measurements yielded $229(30) \text{ cm}^{-1}$ for this fundamental frequency.

Attempts were once more made to assign the first excited state of the C–N torsional mode, but they were futile presumably because of its weakness.

Many ground, as well as excited state lines, were scrutinized for ^{14}N quadrupole splitting. Shoulders were seen on the high-frequency side of several low *J*, *Q*-branch, *c*-type transitions, but it was not possible to resolve them, indicating that the splittings were definitely less than 0.6 MHz. χ_{aa} and χ_{bb} were predicted to be about -1.6 and 1.1 MHz, respectively, using the same assumptions as discussed above in the section of quadrupole determination for conformation I. These values predict small quadrupole splittings and the observed shape of the unresolved, but quadrupole perturbed *Q*-branch, *c*-type lines.

Dipole moment of II. The dipole moment of II was determined in the same manner as described for conformation I. The results are shown in Table 7. The reasonably good agreement between these experimental principal axes dipole moment components and the ones calculated (see above) by the bond-moment method strongly indicates that this is indeed conformation II.

The rotational constants of the hypothetical conformation III and those of either I or II are

Table 7. Stark coefficients^a and dipole moment of conformation II of (aminomethyl)cyclopropane.

Transition		$\Delta\nu/E^2$ (MHz $\text{V}^{-2}\text{cm}^2 \times 10^6$)	
		Obs.	Calc.
$2_{1,1} \rightarrow 3_{1,2}$	$M=0$	$-0.459(8)$	-0.483
	$M=1$	$-6.49(6)$	-6.63
	$M=2$	$-26.1(4)$	-25.2
$2_{0,2} \rightarrow 3_{0,3}$	$M=1$	$-1.12(1)$	-1.07
	$M=2$	$7.00(9)$	7.06
$3_{1,3} \rightarrow 4_{1,4}$	$M=0$	$-0.760(9)$	-0.788
	$M=2$	$1.82(2)$	1.79
	$M=3$	$5.00(5)$	5.02

Dipole moment

$\mu_a=1.018(26)$ D; $\mu_b=0.39(16)$ D; $\mu_c=0.833(55)$; $\mu_{\text{tot.}}=1.372(60)$ D.

^a Uncertainties represent one standard deviation.

not expected to differ very much. The principal-axes dipole moment components of rotamer III were predicted to be $\mu_a=0.8$ D, $\mu_b=0.8$ D and $\mu_c=0.5$ D, respectively, using the bond-moment method. This is very different from those of I ($\mu_a=0.144(2)$ D, $\mu_b \sim 0$ D and $\mu_c=1.077(16)$ D) as shown above. They are also quite different from those of II ($\mu_a=1.018(26)$ D, $\mu_b=0.39(16)$ D and $\mu_c=0.833(55)$ D; Table 7).

The principal axes quadrupole coupling constants of the hypothetical conformation III were predicted to be $\chi_{aa}=1.7$ MHz and $\chi_{bb}=-3.0$ MHz, using the same assumptions as discussed above. This is very different from those observed for I as can be seen from Table 4. The predicted values of χ_{aa} and χ_{bb} of the hypothetical rotamer III should lead to splittings large enough to be well resolved. It is to be remembered that no splittings, only characteristic "shoulders" were seen for some of the lines of II. Based on evidence from the dipole moment components and quadrupole coupling constants, we are confident that the two conformations assigned in this work are indeed I and II shown in Fig. 2. It is most unlikely that one of them has been confused with III.

Searches for further conformations. The assignments made as described above include about 650 transitions. Every strong line of the spectrum has been identified. The great majority of lines of intermediate intensities and many weak transitions have also been assigned. Careful Stark effect studies were made for the majority of the remaining unassigned lines of intermediate intensities. In none of these cases was a well resolved Stark pattern seen.

Searches were also made in an attempt to assign the hypothetical conformation III. The *a*- and *b*-type lines of this rotamer were first looked for since the corresponding dipole moment components are predicted to be larger (see above) than μ_c . However, no assignments were made for these two types of lines. Searches for *c*-type lines were also negative.

The rotational constants of the hypothetical conformations IV and V were then both predicted to be approximately $A=9.0$ GHz, $B=4.2$ GHz and $C=3.8$ GHz. The dipole moment components were predicted to be $\mu_a=1.1$ D, $\mu_b=0.6$ D and $\mu_c=0$ D (for symmetry reasons) for rotamer IV and $\mu_a=0.7$ D, $\mu_b=0$ D and $\mu_c=0.8$ D for V, utilizing the bond-moment method. Sear-

ches among the relatively few unassigned lines of intermediate intensity for an assignment of either IV or V were negative.

Typically the most intense unassigned lines had roughly 15 % of the intensities of the strongest (and identified) lines of the spectrum. If these unassigned transitions were really the spectra of III, IV, and/or V, each of them could not for intensity reasons be present in concentrations exceeding roughly 15 % of I or II. It is thus concluded that conformations I and II are each at least 3 kJ/mol more stable than anyone of III, IV or V. Furthermore, it is believed that the unidentified lines are high J transitions as judged by their unresolved Stark effects. It is considered more probable that these unidentified lines belong rather to unassigned vibrationally excited states of I or II because of their spectral positions and Stark effects, than to further unidentified conformations. The limit of 3 kJ/mol should thus be considered as a conservative estimate. Conformations I and II together thus make up at least 85 % of the gas at about -50°C .

Energy difference between I and II. Intensity comparisons were made for several selected, well-isolated, strong lines belonging to the two identified conformations. Harrington's technique of power saturating the transitions¹² as well as the ordinary use of completely unsaturated lines¹³ were employed.¹⁴ The energy difference was found to be identical within the uncertainty limits with both these methods. The internal energy difference, $\Delta E_0^{\circ} = E_{\text{II}}^{\circ} - E_{\text{I}}^{\circ}$ between I and II was found very precisely as 0.1 kJ/mol with one standard deviation of 0.2 kJ/mol. I is the slightly more stable conformation.

Structure. Only one isotopic species was studied for both conformations and only three rotational constants are thus available for each of them. A complete geometrical structure cannot, therefore, be determined for the two rotamers. A selection of parameters to be fitted must be made. The heavy-atom dihedral angle involving the bisector of the cyclopropyl and the C-C-N link of atoms as well as the C-C-N angle were chosen because the rotational constants are sensitive to variation in these two parameters, they are among the structural parameters most prone to change from one conformation to another, and they are chemically interesting. Further structural parameters likely to vary among various rotamers, namely the

H-N-C-C dihedral angle as well as the H-N-H and H-N-C angles cannot be accurately fitted because the rotational constants are relatively insensitive to variation in these angles. Here, isotopic substitution would have been necessary. The amino group was hence assumed to be in exactly staggered positions in both I and II. The bond lengths and angles which are shown in Table 8 and kept fixed in the fitting procedure, were taken from recent accurate studies of related compounds.

The heavy-atom dihedral angle was varied in steps of one degree and the C-C-N angle in steps of 0.5 degree. The dihedral angles were found as $59(3)^{\circ}$ from *anti* [161(3)^o] from *gauche*; (see Fig. 1) in I and $62(3)^{\circ}$ from *anti* [158(3)g] from *gauche*) in II, and the C-C-N angle as $110.0(15)^{\circ}$ in I, and opening up to $116.0(15)^{\circ}$ in II, respectively. These geometries reproduce the corresponding rotational constants well, as can be seen in Table 8. The error limits have been derived taking into account the inherent uncertainties of the assumed structural parameters.

DISCUSSION

Weak intramolecular hydrogen bonding is possible for all five conformations shown in Fig. 2. The lone electron pair of the nitrogen atom in the hypothetical conformations III and V is oriented such that it would probably be repelled by the pseudo- π electrons in these two forms. Such repulsion is not possible in I, II and the hypothetical conformation IV. It is therefore believed that the hypothetical conformations III and V would be less stable than the other three forms of Fig. 2.

The reason why conformations I and II each are also at least 3 kJ/mol more stable than the hypothetical conformation IV presumably has to do with the more favourable hydrogen bonding situation found in these two conformations. The N-H_a and C_a-C _{β} bonds (Fig. 2) are 26° from being parallel in both I and II as shown in Table 8. A situation in which these two bonds were parallel would presumably have been ideal for an attractive interaction with the pseudo- π electrons of the ring. Moreover, the N-H_a bonds of I and II are lying much closer to the plane of cyclopropane ring, than N-H_c or N-H_{c'} bonds of IV would have been lying. According to the Walsh model of cyclopropane,⁵ the maximum electron

Table 8. Plausible structural parameters^a (bond lengths in pm, angles in degrees) and observed and calculated rotational constants of conformations I and II of (aminomethyl)cyclopropane.

Assumed structural parameters common for I and II					
$C_{\text{ring}}-C_{\text{ring}}$	151.2	$\angle C_{\text{ring}}-C_{\text{ring}}-C_{\text{ring}}$	60.0	$\angle H-N-C-C$ 60 or 180 from <i>syn</i>	
$C_{\text{ring}}-C_{\text{methylene}}$	152.0	$\angle H-C_{\text{ring}}-H^b$	116.0		
$C-N$	147.2	$\angle H-C_{\text{ring}}-C_{\text{methylene}}^b$	116.0		
$C_{\text{ring}}-H_{\text{ring}}$	108.3	$\angle H-C_{\text{methylene}}-H$	109.47		
$C_{\text{methylene}}-H$	109.3	$\angle H-C_{\text{methylene}}-C_{\text{ring}}$	109.47		
$N-H$	101.7	$\angle C-N-H$	109.47		
		$\angle H-N-H$	109.47		
Fitted structural parameters					
		Conformation I		Conformation II	
Heavy-atom dihedral angle		59(3) from <i>anti</i>		62(3) from <i>anti</i>	
$\angle C-C-N$		110.0(15)		116.0(15)	
Rotational constants (MHz)					
Conformation I			Conformation II		
Obs.	Calc.	Diff. (%)	Obs.	Calc.	Diff. (%)
12292.33	12275.13	0.14	12173.18	12191.89	0.15
3202.95	3198.29	0.15	3162.66	3150.93	0.37
2865.80	2872.08	0.22	2846.81	2852.35	0.19
Hydrogen bond parameters					
		Conformation I		Conformation II	
		H_a^c	H_a^c	H_b^c	
$H \cdots C_\alpha$		265	276	276	
$H \cdots C_\beta$		302	312	377	
$N \cdots C_\alpha$		245	254	254	
$N \cdots C_\beta$		330	337	337	
$\angle N-H \cdots C_\alpha$		68	67	67	
$\angle N-H \cdots C_\beta$		97	95	60	
$\angle H \cdots C_\alpha-C_\beta$		89	89	121	
$\angle H \cdots C_\beta-C_\alpha$		61	62	39	
$\angle N-H \cdots C_\alpha-C_\beta^d$		26	26	60	
Sum of van der Waals radii ^e					
$H \cdots C^f$		290	$C \cdots N^f$	320	

^a See text. ^b This angle bisects the $C_{\text{ring}}-C_{\text{ring}}-C_{\text{ring}}$ angle. ^c Atom engaged in internal hydrogen bonding. ^d Angle between $N-H$ bond engaged in hydrogen bonding and closest $C-C$ bond of ring. ^e Taken from Ref. 15. ^f van der Waals radius of carbon taken to be 170 pm as in aromatic systems.

density of the pseudo- π electrons occurs in the plane of the ring. The pseudo- π electrons may thus interact more strongly with the $N-H_a$ bonds of I and II than would have been possible for the $N-H_c$ or $N-H_c'$ bonds. This is believed to be the major reason why (aminomethyl)cyclopropane prefers I and II to the hypothetical conformation IV.

The hydrogen bond cannot be very strong because the $H_a \cdots C_\alpha$ (and $H_b \cdots C_\alpha$ in II) are only slightly shorter than the sum of the van der Waals radii of aromatic carbon and hydrogen as can be seen in Table 8.

In conformation II, not only H_a but also H_b is engaged in hydrogen bonding. However, the contribution from H_b is presumably much less

than from H_a because the $N-H_b$ bond is oriented less favourably relative to the pseudo- π electrons than $N-H_a$ is, as can be seen from the hydrogen bond parameters of Table 8.

The fact that conformations I and II are very close in energy appears to be typical for many amines possessing hydrogen bonds,^{10,11} e.g. $H_2NCH_2CH_2NH_2$,¹⁶ $FCH_2CH_2NH_2$,⁸ $N\equiv CCH_2CH_2NH_2$,¹¹ and $F_2CHCH_2NH_2$.¹⁷ In other cases, only one hydrogen-bonded conformation with the amino group acting as proton donor has been found, e.g. for $CF_3CH_2NH_2$,¹⁸ $H_2NCH_2C\equiv N$,¹⁹ $H_2NCH_2C\equiv CH$, H_2NCH_2COOH ,²⁰ $CH_3OCH_2CH_2NH_2$,²¹ and 2-aminomethyltetrahydropyrene.²²

The heavy-atom dihedral angles correspond to nearly staggered atomic arrangement, and such geometries have also been found for the other hydrogen-bonded amines.^{10,11,16-22} The $C-C-N$ angle opens up by 6° from I to II. Other amines having an amino-group geometry similar to conformation II are all characterized by having a $C-C-N$ angle typically $4-6^\circ$ larger than in the cases corresponding to I.^{10,11} 1,3-repulsive interaction may be the reason for this angle opening.

REFERENCES

- Schei, S. H. *Acta Chem. Scand. A* 37 (1983) 15 and references therein.
- Fujiwara, F. G., Chang, J. C. and Kim, H. J. *Mol. Struct.* 41 (1977) 177.
- Mohammadi, M. A. and Brooks, W. V. F. *J. Mol. Spectrosc.* 77 (1979) 42.
- a. Bhaumik, A., Brooks, W. V. F., Dass, S. C. and Sastry, K. V. L. N. *Can. J. Chem.* 48 (1970) 2949; b. Brooks, W. V. F. and Sastri, C. K. *Can. J. Chem.* 56 (1978) 530.
- Walsh, A. D. *Trans Faraday Soc.* 45 (1949) 179.
- Smyth, C. P. *Dielectric Behaviour and Structure*, McGraw-Hill, New York 1955, p. 244.
- Esbitt, A. S. and Wilson, E. B., Jr. *Rev. Sci. Instrum.* 34 (1963) 901.
- Marstokk, K.-M. and Møllendal, H. *Acta Chem. Scand. A* 34 (1980) 15.
- a. Gordy, W. and Cook, R. L. *Microwave Molecular Spectra*, Interscience, New York 1970, p. 262; b. *Ibid.* p. 267.
- Møllendal, H. *J. Mol. Struct.* 97 (1983) 303.
- Braathen, O.-A., Marstokk, K.-M. and Møllendal, H. *Acta Chem. Scand. A* 37 (1983) 493.
- a. Harrington, H. W. *J. Chem. Phys.* 46 (1967) 3698; b. *Ibid.* 49 (1968) 3023.
- Townes, C. H. and Schawlow, A. L. *Microwave Spectroscopy*, McGraw-Hill, New York 1955, p. 372.
- Wilson, E. B., Jr., Caminati, W. and Møllendal, H. *To be published*.
- Pauling, L. *The Nature of the Chemical Bond*, 3rd. Ed., Cornell University Press, New York 1960, p. 260.
- Marstokk, K.-M. and Møllendal, H. *J. Mol. Struct.* 49 (1978) 221.
- Marstokk, K.-M. and Møllendal, H. *Acta Chem. Scand. A* 36 (1982) 517.
- Warren, J. D. and Wilson, E. B., Jr. *J. Chem., Phys.* 65 (1972) 2137.
- Pickett, H. M. *J. Mol. Spectrosc.* 46 (1973) 335.
- Suenram, R. D. and Lovas, F. J. *J. Am. Chem. Soc.* 102 (1980) 7180.
- Caminati, W. and Wilson, E. B., Jr. *J. Mol. Spectrosc.* 81 (1980) 356.
- Turner, P. H. *J. Am. Chem. Soc.* 101 (1979) 4499.

Received October 24, 1983.